ELSEVIER

Contents lists available at ScienceDirect

Weather and Climate Extremes

journal homepage: www.elsevier.com/locate/wace





The role of compound climate and weather extreme events in creating socio-economic impacts in South Florida

Javed Ali ^{a,b,*}, Thomas Wahl ^{a,b}, Alejandra R. Enriquez ^{a,b,c}, Md Mamunur Rashid ^d, Joao Morim ^{a,b}, Melanie Gall ^e, Christopher T. Emrich ^{b,f}

- ^a Department of Civil, Environmental and Construction Engineering, University of Central Florida, Orlando, FL, 32816, USA
- ^b National Center for Integrated Coastal Research, University of Central Florida, Orlando, FL, 32816, USA
- ^c Institute for Environmental Studies (IVM). Vrije Universiteit Amsterdam, 1081 HV Amsterdam, the Netherlands
- d Division of Coastal Sciences, School of Ocean Science and Engineering, University of Southern Mississippi, Ocean Springs, MS, 39564, USA
- ^e Center for Emergency Management and Homeland Security, School of Public Affairs, Arizona State University, Phoenix, AZ, 85004, USA
- ^f School of Public Administration, University of Central Florida, Orlando, FL, 32816, USA

ABSTRACT

Natural hazards such as hurricanes, floods, and wildfires cause devastating socio-economic impacts on communities. In South Florida, most of these hazards are becoming increasingly frequent and severe because of the warming climate, and changes in vulnerability and exposure, resulting in significant damage to infrastructure, homes, and businesses. To better understand the drivers of these impacts, we developed a bottom-up impact-based methodology that takes into account all relevant drivers for different types of hazards. We identify the specific drivers that co-occurred with socio-economic impacts and determine whether these extreme events were caused by single or multiple hydrometeorological drivers (i.e., compound events). We consider six types of natural hazards: hurricanes, severe storm/thunderstorms, floods, heatwaves, wildfire, and winter weather. Using historical, socio-economic loss data along with observations and reanalysis data for hydrometeorological drivers, we analyze how often these drivers contributed to the impacts of natural hazards in South Florida. We find that for each type of hazard, the relative importance of the drivers varies depending on the severity of the event. For example, wind speed is a key driver of the socio-economic impacts of hurricanes, while precipitation is a key driver of the impacts of flooding. We find that most of the high-impact events in South Florida were compound events, where multiple drivers contributed to the occurrences and impacts of the events. For example, more than 50% of the recorded flooding events were compound events and these contributed to 99% of total property damages and 98% of total crop damages associated with flooding in Miami-Dade County. Our results provide valuable insights into the drivers of natural hazard impacts in South Florida and can inform the development of more effective risk reduction strategies for improving the preparedness and resilience of the region against extreme events. Our bottom-up impact-based methodology can be applied

1. Introduction

Natural hazards such as floods, hurricanes, heatwaves, and wildfires cause significant economic losses as well as a high number of fatalities worldwide (World Economic Forum, 2023; NOAA 2023; WMO 2023). Natural hazards are environmental phenomena causing societal and environmental impacts, while hydrometeorological variables are defined as the drivers that may cause natural hazards (FEMA n.d.). Natural hazards are often caused by hydrometeorological drivers which may include processes, variables, and phenomena in the climate and weather domain and can span over multiple spatial and temporal scales. Since 1980, the United States has experienced more than 330 weather and climatic disasters exceeding USD 1 billion in damage each, tallying to more than USD 2.275 trillion in direct insured and uninsured costs

(NOAA NCEI, 2022). NOAA's Billion-Dollar events include indirect losses, flood insurance payouts, and more. However, hazards and disasters, including compound events, do not need to exceed the arbitrary one-billion-dollar threshold to be catastrophic to a community. A more conservative estimate of direct hazard losses alone, still shows a tally of nearly USD 1.2 trillion in direct losses, nearly 35,300 fatalities, and over 252,000 injuries since 1960 in the United States—across all types of natural hazards (CEMHS 2022). Many of these events as well as the billion-dollar disasters might be compound events meaning a combination of multiple drivers and/or hazards that collectively cause extreme and/or catastrophic damage to society and the environment (McPhillips et al., 2018; Zscheischler et al., 2018). The share of compound events especially among high-impact events, though, is unknown at this point.

^{*} Corresponding author. Department of Civil, Environmental and Construction Engineering, University of Central Florida, Orlando, FL, 32816 USA. E-mail address: javed.ali@ucf.edu (J. Ali).

In the United States, the socio-economic cost of weather- and climate-related disasters has significantly grown over the last 50 years (NOAA NCEI, 2023). In coastal areas such as Florida, with low-lying and densely populated coastal cities, climate-related hazards can be catastrophic as the devastating impacts of Hurricane Ian underscored. Hurricane Ian (2022) made landfall as category 4, being the third-costliest ever weather disaster on record globally, and was the deadliest hurricane to hit the state of Florida since the 1935 Labor Day hurricane (Masters and Henson, 2023).

In the near future, Florida may see more hurricanes and severe weather. The 6th Assessment Report of the Intergovernmental Panel on Climate Change (IPCC) projects future changes in mean sea level, extreme temperatures, extreme precipitation, river flow, fire weather, tropical cyclone activity, and severe winds, among others, in Florida (Seneviratne et al., 2022). In a warming climate, the dependence and hence interaction effects between different climatic drivers may change (Yaddanapudi et al., 2022; Zscheischler et al., 2018), and because of these expected future changes, it is essential to develop a baseline understanding of disaster risks, particularly for high-impact compound extreme events. As a result, it is critical to understand the processes driving these extreme events, as well as how various hydrometeorological drivers combine to contribute to the associated socio-economic impacts. Traditional risk assessments study the intensity, frequency, and impact of singular hazards and/or climate drivers, such as temperature, precipitation, river discharge, sea level, wind, etc. (Chen et al., 2022; Deng and Ritchie, 2019; Hirabayashi et al., 2021; Kharin et al., 2013; Klaus et al., 2016; Lenderink et al., 2007; Perkins and Alexander, 2013; Veatch and Villarini, 2020; Ward et al., 2020). The univariate approach leads at best to uncertainty in the risk assessment outcomes, and at worst to a systematic underestimation of potential impacts, which consequently results in ineffective, maladaptive, and/or under-designed risk mitigation action (Zscheischler et al., 2018; Schipper, 2020). Thus, the design and implementation of the right-sized and effective adaptation strategies rely on a comprehensive understanding of the climatic and meteorological drivers relevant to a particular area and their compounding effects.

Compound events are complex multivariate phenomena with nonlinear interactions between varying spatial and temporal physical and societal mechanisms. Hence, their impacts are often amplified relative to the impacts from those same climate events occurring separately or univariately (Raymond et al., 2020a,b). Impacts from hurricanes, for example, typically result from concurrent hazards such as extreme precipitation, winds, and high storm surge. For instance, Hurricane Ian (2022) caused more than 20 inches (~51 cm) of total precipitation in some places, maximum sustained winds of 155 mph (~250 km/h), and storm surge heights of 12-18 feet (3.66-5.5 m) in Florida, leading to economic losses of at least USD 113 billion and killing at least 152 people (NOAA NCEI, 2023). Severe damage can also result from a series of smaller magnitude (or extreme) weather events that exacerbate system vulnerability or result in disproportionate impacts (Moftakhari et al., 2019; Bevacqua et al., 2022a,b). For instance, in 2022, the U.S. experienced a billion-dollar disaster related to flooding in Missouri and Kentucky. The flooding was caused by a series of storms that dumped record amounts of rain in the region in March 2022. The flooding affected more than 1.5 million people and damaged or destroyed over 20,000 homes (NOAA NCEI 2022). Capturing these complex interrelationships is a challenge for current physics-based modeling approaches, scenario-building techniques, and statistical analyses (Zscheischler et al., 2018). A recently proposed typology of compound events underscores the necessity for impact-based methods that identify multiple weather and climatic drivers leading to socio-economic risk (Zscheischler et al., 2020). Applications within the disaster risk reduction cycle usually fail to take into account compound drivers and impacts, which can result in a misrepresentation of risk, ineffective emergency response, or improper adaptation of multiple actions across the disaster risk management cycle (Matanó et al., 2022; Simpson et al.,

2023; van den Hurk et al., 2023). To overcome this shortcoming, innovative approaches are emerging that couple risks from multiple threats (Sadegh et al., 2018). Most of these approaches, though, represent advances in statistical risk modeling and risk estimation with the likelihood of hazard(s) occurrence as the central focus. The necessity to analyze compound hazards, their drivers, and their impacts has recently been highlighted in the literature (AghaKouchak et al., 2020; Ward et al., 2022).

Previous studies on compound events have applied statistical and probabilistic methods to obtain the joint dependence between predefined combinations of drivers, which implies certain subjectivity (Bevacqua et al., 2021; Camus et al., 2022; Hao et al., 2018; Leonard et al., 2014; Ridder et al., 2022; Wahl et al., 2015). Statistical dependence has been found between multiple hazards and climate drivers such as precipitation and wind extremes (Martius et al., 2016), river discharge and surge (Moftakhari et al., 2019; Serafin et al., 2019) as well as precipitation and temperature (Bevacqua et al., 2022a,b; Rashid and Wahl, 2022), the latter leading to a negative correlation that potentially results in drought, heatwaves, and fires (Matthews and Marston, 2019; Raymond et al., 2020a,b; Sutanto et al., 2020; Zscheischler and Seneviratne, 2017). Other dependencies have also been identified between flooding drivers such as heavy rainfall and storm surge over different spatial scales (Bevacqua et al., 2019; Hendry et al., 2019; van den Hurk et al., 2015; Wu et al., 2018), with previous works showing that neglecting even weak dependencies can result in the underestimation of coastal extreme water levels (Ikeuchi et al., 2017; Zheng et al., 2014) leading to a miscalculation of flooding risk (Lian et al., 2013; Zheng et al., 2013).

The characteristics of hydrometeorological hazards (frequency, magnitude) and climate drivers change spatially, and so do their dependencies. Thus, site-specific analysis is needed. For example, Couasnon et al. (2020) analyzed the correlation between storm surge and river discharge globally using simulated data. They found a significant positive correlation in many regions including the Miami-Dade County area in southeast Florida (our case study). Jane et al. (2020) also found significant correlation between extreme rainfall, ocean water level (tide + non-tidal residual), and groundwater level from in-situ observations in Miami-Dade. For most catchments in southeast Florida, the combination of heavy rainfall and high antecedent soil moisture is the major flood-generating process (Berghuijs et al., 2016; Jane et al., 2020). In addition, Zscheischler and Seneviratne (2017) assessed the co-occurrence of hot and dry summers globally and found a high negative correlation between temperature and precipitation over the warmest three months in many regions across the globe, including South Florida. These findings point at an urgency that current risk assessment and management procedures are adjusted to consider potential combinations of high-impact drivers, in the face of a growing number of compound extreme events.

This paper moves beyond joint distribution functions and instead uses atmospheric re-analysis and historical observational data for hydrometeorological drivers of natural hazards along with empirical loss information including property and crop damage as well as injuries and fatalities to link all hydrometeorological drivers to impactful events in Miami-Dade County. The goal of this study is to analyze: a) what role compound events played in generating historic socio-economic losses, and b) which hydrometeorological drivers created these compound events and their associated adverse effects. More specifically for Miami-Date County, we investigate, for example, if flooding events occurred as a result of excessive precipitation alone or in combination with additional hazards and drivers like storm surge, river discharge, and soil moisture. We also assess how much damage compound flood events caused compared to the univariate events and which drivers were involved in creating compound events. By using site-specific exposure data, we implicitly account for the built environment of the area. Results provide guidance on the multi-driver association and high-impact events thereby establishing a baseline to identify and monitor future changes.

Going forward, this novel methodology can be applied in any location to understand the contributions of different drivers to the impacts of natural hazards, and the results may enable stakeholders to make science-informed decisions when planning disaster response and adaptation measures.

2. Study area

Miami-Dade County (Fig. 1), a low-lying coastal county located in southeast Florida, is the 9th largest county in the United States with a population of more than 2.7 million (as of the 2020 census) (United States Census Bureau, 2021). The most populous county in the State of Florida, Miami-Dade is projected to reach 3.2 million inhabitants by 2030 (Seijas et al., 2011).

Miami-Dade's costliest flood event (in the SHELDUS database; see section 3.1 for more information on SHELDUS) on record (which was a declared disaster) occurred in October of 2000. A tropical storm system produced a 10-mile-wide swath of 10–20 inches of rain across southeast Florida (NOAA, 2022) resulting in direct losses exceeding USD 662 million in property damage and USD 752 million in crop damage (CEMHS, 2020). Also, during the devastating 2003 Atlantic hurricane season, flooding damage to critical infrastructure and properties topped USD 100 billion across the impacted region, with Miami-Dade County among the most affected areas (Lawrence et al., 2005).

In 2007, the Organization for Economic Cooperation and Development (OECD) identified Miami-Dade County as the area with the highest amount of vulnerable assets exposed to coastal flooding by the 2070s globally, with projected annual costs of approximately USD 3.5 trillion (Nicholls et al., 2007). In a warming world, Miami-Dade County will likely experience not only sea-level rise but also changes in precipitation patterns and temperature extremes (Karl et al., 2009; Nakićenović and Swart, 2000; Seneviratne et al., 2022). This increases the likelihood of flooding, heatwaves, and droughts with detrimental effects on humans, the environment, and built infrastructure. Sea-level rise alone, which is one of the most certain consequences of a warming climate, is expected to lead to an increase in the frequency of high tide flooding, storm surge damage, population displacement, damage to infrastructure, saltwater intrusion, and the spread of infectious diseases. Furthermore, the combination of storm surge inundation and high wind impacts from tropical storms poses additional challenges for coastal areas such as Miami-Dade County.

3. Data

3.1. Socio-economic impact data

This study leverages direct loss information from the Spatial Hazard Events and Losses Database for the United States (SHELDUS Version 19) (CEMHS, 2020). Direct loss information includes property damage, crop damage, injuries, and fatalities caused by natural hazards. Loss records are georeferenced to county-level. SHELDUS Version 19 comprises nearly 926,000 records spanning 1960–2019. While loss estimates of many hydrometeorological hazard events originate from NOAA's National Centers for Environmental Information (NCEI) Storm Events reports, SHELDUS conducts post-processing on multi-county events (either reported as a list of affected counties or so-called forecast zones) to assign losses (or loss shares) to affected counties (CEMHS, 2022). For Miami-Dade County, SHELDUS reported 335 loss events associated with 11 distinct types of hazards (Table 1). All property and crop damages were inflation-adjusted to 2019 U.S. dollars up to 2 decimal places. Note

Table 1
List of SHELDUS hazards along with indication ("Yes"/"No") of their occurrence in Miami-Dade County and whether they are considered in the analysis. Numbers in brackets indicate the total number of events of this particular hazard between 1979 and 2019.

Hazards in SHELDUS	Hazards in Miami-Dade County	Included in analysis	Included as hazard	Included as driver
Flood	Yes (37)	Yes	Yes	No
Hurricane/ Tropical storm	Yes (24)	Yes	Yes	No
Drought	N/A (0)	N/A	N/A	N/A
Severe storm/ Thunderstorm	Yes (67) ^a	Yes	Yes	No
Wildfire	Yes (4)	Yes	Yes	No
Heat	Yes (4)	Yes	Yes	No
Coastal	Yes (43)	No	No	No
Winter weather	Yes (9) ^b	Yes	Yes	No
Tornado	Yes (29) ^c	Yes	No	Yes
Hail	Yes (6) ^d	Yes	No	Yes
Fog	N/A	N/A	N/A	N/A
Lightning	Yes (68)	Yes	No	Yes
Wind	Yes (65) ^e	Yes	No	Yes

- ^a In some cases, Wind and Hail were also reported..
- $^{\rm b}$ In two cases, Wind was also reported..
- ^c In one instance, Wind was also reported..
- $^{\rm d}\,$ In a few cases, Wind and Severe Storm/Thunderstorm were also reported.
- $^{\rm e}$ In some cases, Severe Storm/Thunderstorm, Hail, Winter Weather and Tornado were also reported..

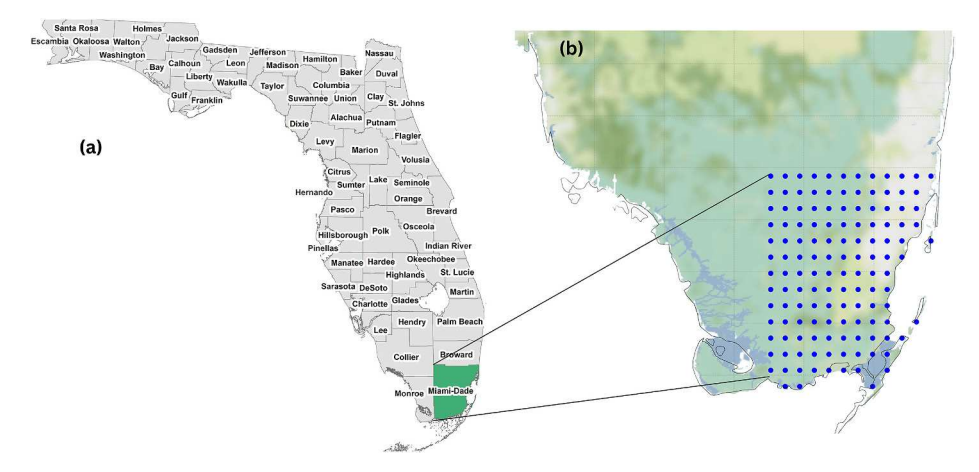


Fig. 1. (a) State of Florida map showing all counties, and the study area, Miami-Dade County (shown in green color), and (b) all locations where hydrometeorological information are available within the study area (shown in blue color).

that SHELDUS underreports the direct losses (property and crop damage) since it takes the lower value of the range of loss if the loss estimate was reported as a range in the original data source. In addition, when an event impacted more than one county, SHELDUS distributes losses equally across the affected counties including injuries and fatalities; that sometimes results into a fraction of injuries and fatalities. Hurricanes inherently incorporate drivers like precipitation and river discharge, both of which can also be associated with flooding events. The distinction between such overlapping events is firmly rooted in the SHELDUS database's specifications. SHELDUS ensures that there are no overlapping entries for both hurricane and flooding events. This means that even if a hurricane might physically cause flooding due to its associated precipitation and river discharge, SHELDUS categorizes and records it distinctly as a hurricane event and not as a flood. This established classification in the SHELDUS database ensures that there is no double-counting or ambiguity in event categorization.

Given the focus of this study, impactful events associated with hazards that are always caused by just one driver were excluded, namely: wind, lightning, hail, and tornado. While those are classified as distinct hazard types in SHELDUS, they are also drivers that contribute to other types of hazards (for instance, wind is a driver within a hurricane). Hence, they are included here in the set of hydrometeorological drivers but not investigated as individual hazards. As a result, we obtained 144 impact entries for six types of hazards (flooding, wildfire, severe storm/thunderstorm, hurricane/tropical storm, winter weather, and heat) for Miami-Dade. Those 144 loss events occurred between 1979 and 2019. Table 2 shows the temporal coverage of hydrometeorological drivers, which is mostly identical to the temporal coverage of loss events.

SHELDUS did not report any loss events for droughts, earthquakes, tsunamis, or landslides for our study area. Loss events classified as "coastal hazards" in SHELDUS were excluded from this study as those records were mostly univariate events caused by high surf or rip ocean currents, resulting in injuries or fatalities on beaches rather than property and crop damage. Rip current impacts (i.e., injuries and/or fatalities) are mostly the product of human behavior and less so the consequence of hydrometeorological drivers; hence, we did not consider "Coastal" as a hazard or driver in the analysis.

3.2. Hydrometeorological data

The data sources for historical observations and atmospheric reanalysis data of 12 hydrometeorological drivers are listed in Table 2. We selected data from 1979 to 2019 due to the limited availability of continuous hydrometeorological data before 1979. The datasets originate from nine different sources with variable spatial and temporal resolutions though they all cover the entire study area (Table 2).

Eight of the hydrometeorological drivers are obtained from different reanalysis datasets. Wind speed (at 10 m), soil moisture (volume of water in soil layer 1: 0–7 cm), and relative humidity are retrieved from ERA5, the fifth generation of the European Centre for Medium-range

Weather Forecast (ECMWF) global reanalysis. ERA5 covers the period from 1979 to present at an hourly resolution and with a spatial resolution of $0.25^{\circ} \times 0.25^{\circ}$. We use Global Flood Awareness Systems (GLoFAS) reanalysis from ECMWF to obtain daily river discharge data from 1979 to 2020 at $0.1^{\circ} \times 0.1^{\circ}$ spatial resolution. Temperature (daily maximum and minimum) is collected from the gridMET climatology lab, which includes daily surface temperature reanalysis data from 1979 to present at $0.042^{\circ} \times 0.042^{\circ}$ spatial resolution. Daily precipitation is obtained from Pierce et al. (2021) for the period 1979 to 2018, gridded at a spatial resolution of $0.0625^{\circ} \times 0.0625^{\circ}$. This is a revised version of the (Livneh et al., 2013) precipitation dataset that omits the time adjustment and is shown to perform significantly better in reproducing extreme precipitation metrics (Pierce et al., 2021). Fire Weather Index (FWI) data is obtained from the Copernicus Emergency Management Service (CEMS), which is developed based on the Canadian Fire Weather Index Rating System and the ECMWF ERA5 reanalysis dataset (Vitolo et al., 2020). The FWI is a numerical measure of potential frontal fire intensity that is a combination of the initial spread index and the build-up index. The FWI system uses temperature, relative humidity, wind speed, and 24-hr precipitation data. Storm surge information is obtained from the Coastal Dataset for the Evaluation of Climate Impact (CoDEC) (Muis et al., 2020). CoDEC is produced by forcing the third-generation Global Tide and Surge Model (GTSM v3.0) with meteorological fields from the ERA5 climate reanalysis (Hersbach et al., 2018) for 1979 to 2018. The model has a resolution of 2.5 km along the U.S. coastline but hourly still water levels are only output for approximately 18,000 locations along the global coastline, which is approximately every 50 km along a smoothed coastline (see Muis et al. (2020) for more details). Compound flood assessments typically focus on the meteorological surge component (instead of still water levels) since there are generally dependencies between storm surge and other drivers though not between tide and other weather-related variables (Eilander et al., 2022; Nasr et al., 2021).

Hail information at daily resolution is retrieved from the National Centers for Environmental Information (NCEI) NOAA radar-based dataset, with a $0.75^{\circ} \times 0.75^{\circ}$ spatial coverage. Hail data contains information of a storm's probability of producing severe sized (diameter 1.9 cm or bigger) hail, the storm's probability of producing hail of any size, and the maximum expected size of that hail, as well as storm locations. Tornado data is acquired from NOAA's Storm Prediction Center. Tornado strength is presently evaluated using the Enhanced Fujita Scale (adopted from the basic Fujita Scale in 2007), which assigns a rating of 0-5 based on expected wind speeds and the severity of the damage. Lightning data is obtained from the United States National Lightning Detection Network (NLDN), a lightning detection network operated by Vaisala company, and data archived by NOAA's National Centers for Environmental Information (NCEI). It provides the number of cloud-toground lightning strikes measured for each day for all counties and states in the U.S.

All hydrometeorological variables are interpolated to a common grid with a resolution of $0.0625^\circ\times0.0625^\circ$ (i.e., approximately 6 km²) to

Table 2 Summary of hydrometeorological data and their sources.

Variable	Spatial resolution	Temporal resolution	Time coverage	Source
1. River discharge	$0.1^{\circ} \times 0.1^{\circ}$	Daily	1979–2019	GLoFAS ECMWF (Harrigan et al., 2021)
2. Wind	$0.25^{\circ} \times 0.25^{\circ}$	Hourly	1979-2019	ERA5 ECMWF (Hersbach et al., 2018)
3. Maximum temperature	$0.042^{\circ} \times 0.042^{\circ}$	Daily	1979-2019	gridMET (Abatzoglou, 2013)
4. Minimum temperature	$0.042^{\circ} \times 0.042^{\circ}$	Daily	1979-2019	gridMET (Abatzoglou, 2013)
5. Precipitation	$0.0625^{\circ} \times 0.0625^{\circ}$	Daily	1979-2018	Non-split Livneh (Pierce et al., 2021)
6. Soil moisture	$0.25^{\circ} \times 0.25^{\circ}$	Hourly	1979-2019	ERA5 ECMWF (Hersbach et al., 2018)
7. Fire weather index	$0.25^{\circ} \times 0.25^{\circ}$	Daily	1979-2019	CEMS ECMWF (Vitolo et al., 2020)
8. Storm surge	2.5-km ^a	Hourly	1979-2018	CODEC (Muis et al., 2020)
9. Lightning	_	Count	1987-2019	U.S. National Lightning Detection Network (NLDN)
10. Hail	$0.75^{\circ} \times 0.75^{\circ}$	Daily	1995-2019	NCEI NOAA
11. Tornado	_	Event-based	1980-2019	NOAA Storm Prediction Center
12. Relative humidity	$0.25^{\circ} \times 0.25^{\circ}$	Hourly	1979-2019	ERA5 ECMWF (Hersbach et al., 2018)

^a Resolution of 2.5 km along the global coast (1.25 km in Europe), resulting in 18,000 model points.

match the scales of the higher resolutions of precipitation, minimum temperature, maximum temperature, and river discharge ($<10\,$ km) which is critical at the county level and to ensure consistency in our analysis that allow for comparisons between different variables. In addition, all offshore grids points are removed. This results in a total of 134 grid points and hence 134 time series for each hydrometeorological variable for Miami-Dade County. Hourly time series of wind, soil moisture, storm surge, and relative humidity are converted to daily maxima. Because information on hurricanes, lightning, storm surge, and hail are not provided in a uniform spatial format, data for those variables are not re-mapped.

4. Methodology

A bottom-up impact-based approach is developed that identifies the drivers that have led to socio-economic impacts in Miami-Dade County and determines which extreme events were caused by multiple hydrometeorological drivers (i.e., whether they were compound or univariate extreme events). First, we identify all relevant hydrometeorological drivers (Table 2) composing each hazard (Table 1) based on expert knowledge and previous studies (AghaKouchak et al., 2020; Bevacqua et al., 2021; Camus et al., 2022; Raymond et al., 2020a,b; Wahl et al., 2015; Zscheischler et al., 2018, 2020) (see Fig. 2). By doing so, we

eliminate spurious correlations between the drivers and unrelated hazard types. For instance, in a wildfire event, hydrometeorological drivers such as river discharge, storm surge, or precipitation are irrelevant and should not be used as predictor variables, despite possibly showing high values somewhere in our study area during the time when an impact was recorded. Note that loss data are only available at the county level and no detailed information is available on where exactly within the county an impact occurred. However, hydrometeorological data have a greater spatial resolution, which provides us with more than one time-series location of each hazard within a county. This means that certain drivers could be extreme somewhere within the county but unrelated to the impact event. The minimum soil moisture is not included as a driver of heat because the heat did not cause any crop and property damage in our study area; but if a similar analysis is conducted elsewhere, where heat created property or crop losses, it would be an interesting driver to include.

Fig. 3 shows the different analysis steps in the proposed framework. Steps (a) and (b) include data acquisition and data processing steps as described above. Subsequently, the percentiles were calculated for each hydrometeorological driver considering the individual time series data for each grid point in our study area for the entire time period, except for hurricanes, lightning, tornado, and hail which are not continuous time-series. Instead, hurricane category, lightning strike count, f-scale of

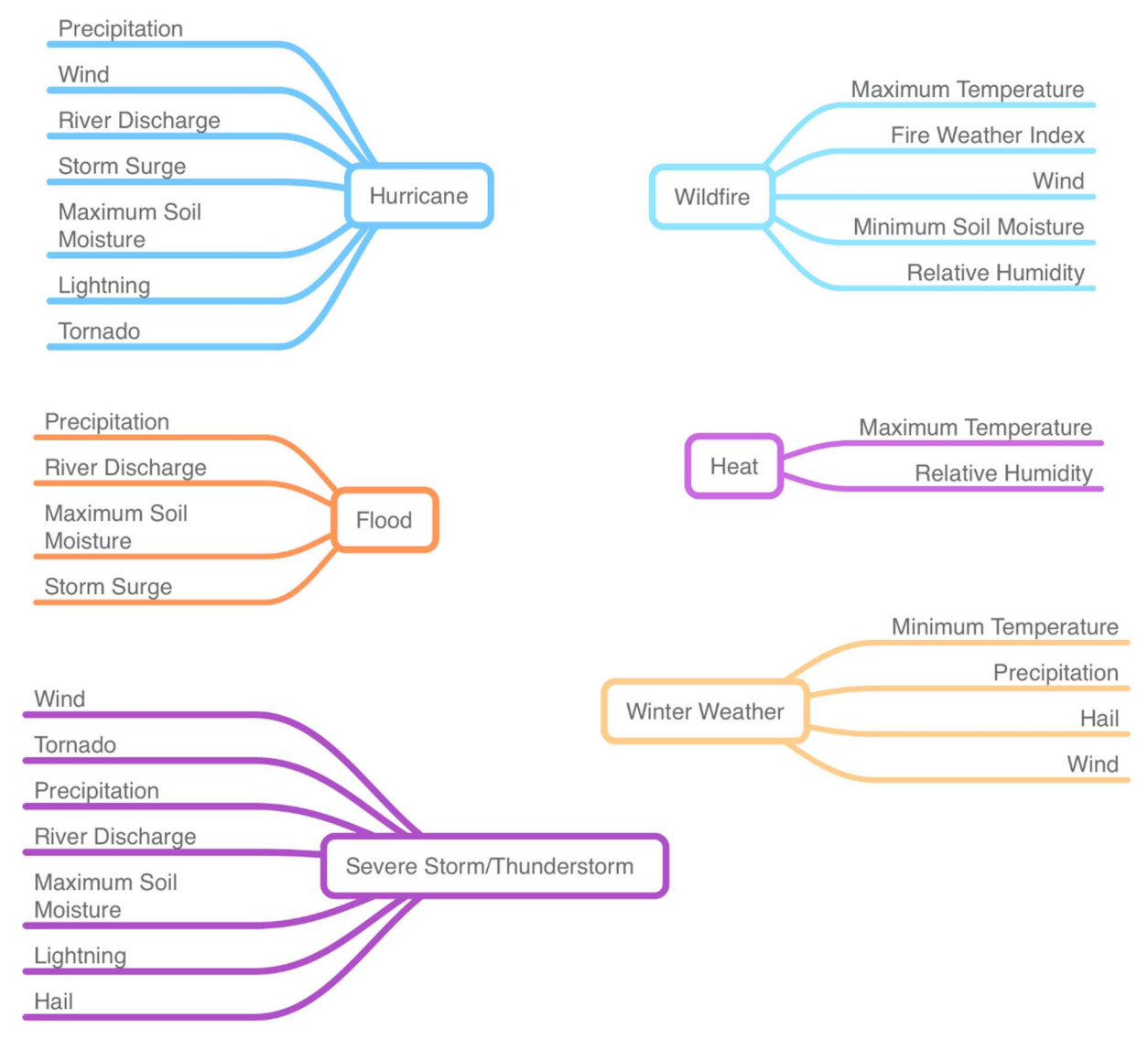


Fig. 2. An overview of all relevant hydrometeorological drivers associated with different types of hazards.

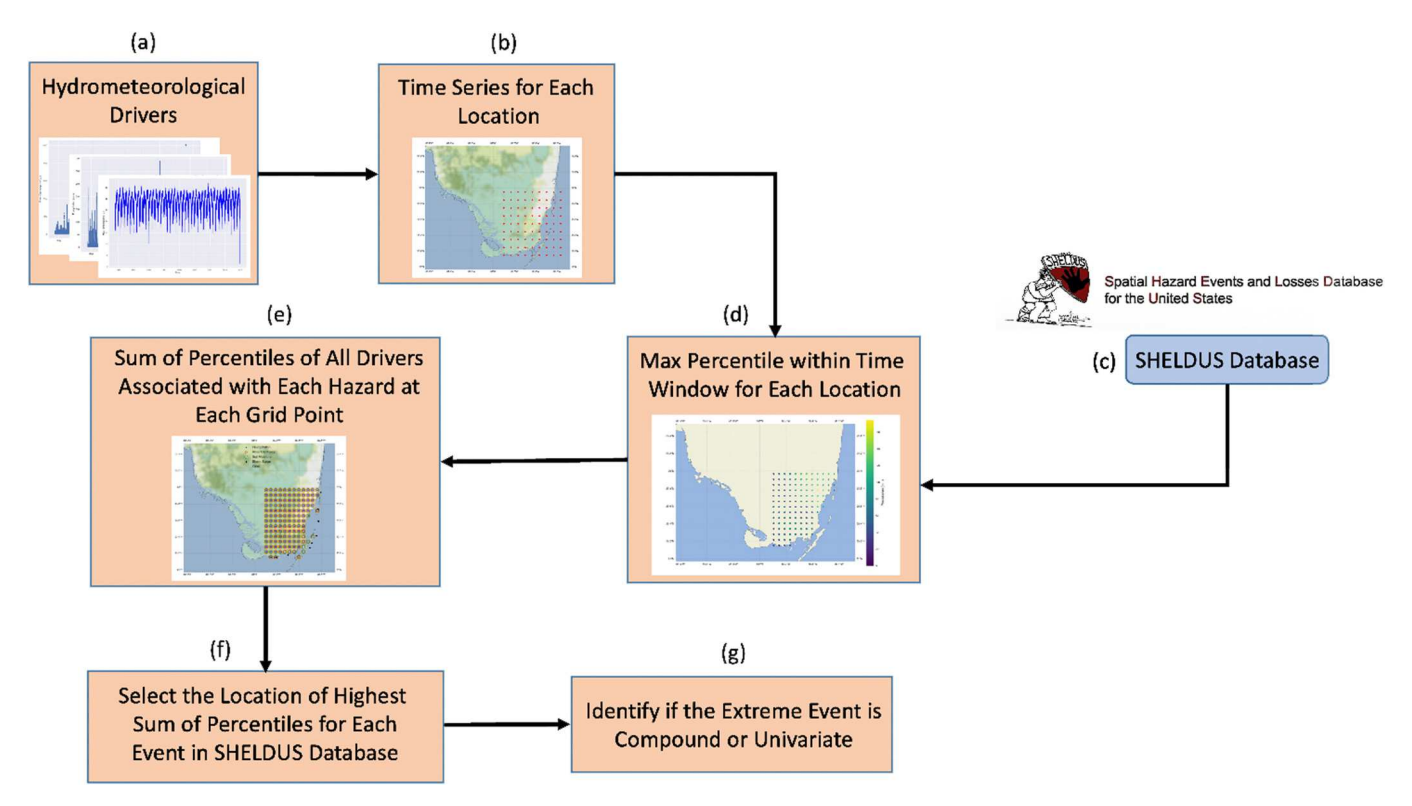


Fig. 3. Framework outlining the steps involved in the proposed methodology.

tornadoes, and severe hail probability, respectively are used. All data are presented as percentiles instead of absolute magnitudes to represent the relative extremeness of the event at each site, thus implicitly acknowledging the adaptabilities and susceptibilities of the built environments and socio-economic conditions in diverse areas. For instance, in a region where high-intensity rainfalls are relatively more frequent, the built environment might be better adapted with superior drainage systems, and the socio-economic systems might have evolved to minimize disruptions from such events. Conversely, in a location where such rainfalls are rare, even a lower magnitude might result in significant disruptions due to the lack of appropriate infrastructure and socio-economic adaptations. By representing the data in percentiles, we are essentially normalizing the events based on their relative frequency and extremeness in each location, which implicitly captures the varying adaptabilities and susceptibilities of different sites, dictated by their built environments and socio-economic conditions. For wildfires, minimum soil moisture is used instead of maximum, i.e., the highest percentiles of soil moisture correspond to the lowest soil moisture content.

We then introduce a SHELDUS derived impact measure to identify when a hazard loss event has occurred (Step c). The impact period, recorded in SHELDUS, is extended by one day in each direction to account for cases where a driver was extreme on one day, but the impact was recorded the next day, and vice versa. Soil moisture is an exception where the time window extends only to one day before the impact since soil moisture is a pre-condition for flooding events (Mahdi El Khalki et al., 2020; Tramblay et al., 2021). Our selection of the ± 1 day window was based on both the spatial and temporal characteristics of the hydrometeorological drivers under study and previous scientific literature. Many hydrometeorological phenomena can significantly influence the environment within this timeframe, and this choice was also guided by research indicating that a 1-day window is a common time frame for examining concurrent weather phenomena (for instance, Zhang et al., 2021; Song et al., 2023).

For each impact entry, the maximum percentiles of all relevant drivers (according to Fig. 2) are estimated (Step d) within the extended impact time window for all grid points. That leads to 134 percentile

values within the study domain for each relevant variable. Next, the percentiles of all the relevant hydrometeorological variables at all grid points are summed up (Step e) and the grid point with the highest sum of percentiles is selected (Step f). In the absence of sub-county impact locations, we assume that impacts registered in SHELDUS occurred in the vicinity of the grid point with the highest sum of percentiles for the drivers linked to the particular hazard. For example, in the case of flooding, four hydrometeorological drivers were identified which can lead or contribute to flooding: precipitation, river discharge, soil moisture, and storm surge (for instance, see Fig. 8). For the first three, we have gridded data across the study area. We add their percentiles at each grid point and assume that the flooding impact occurred where the sum is highest. This summed percentile approach not only highlights regions with the most extreme individual drivers but also underscores locations where the combined influence of multiple drivers can contribute to heightened event severity, even if not all drivers surpass the 95th percentile. For storm surge, we selected the percentile value from the nearest coastal grid point that is spatially aligned with the location displaying the highest combined percentiles of the other three hydrometeorological drivers for flooding.

For the purpose of this study, we consider an event to be compound when at least two of the hydrometeorological drivers linked to a given hazard type exceeded their respective 95th percentile thresholds. In Step (g), all impactful extreme events are analyzed to determine if they were compound or univariate events. Note that hurricane category and tornado's f-scale are not included in defining the compound events. Rather, we utilize these metrics to illustrate the impact of various hurricane categories on the region and to gauge the severity of any tornadoes using the f-scale. A sensitivity analysis is also performed using the 90th and 99th percentile thresholds to define compound events (in addition to the 95th).

5. Results

As described previously, a total of six hazard types were identified for Miami-Dade County based on the hazard selection criteria: flooding, wildfire, heat, hurricane/tropical storm, winter weather, and severe storm/thunderstorm. Each hazard type was linked to their most relevant hydrometeorological drivers (Fig. 2) out of 12 candidate variables: river discharge, precipitation, soil moisture, storm surge, wind, fire weather index, maximum temperature, minimum temperature, relative humidity, hail, lightning, and tornado.

Between 1979 and 2019, hurricanes resulted in the highest economic losses in Miami-Dade County with at least USD 13.53 billion (USD 12.04 billion property damage and USD 1.49 billion crop damage), followed by flooding with a total of at least USD 1.905 billion (USD 821M property damage and USD 1.08B crop damage), and winter weather with a total of at least USD 381.3M (USD 36.58M property damage and USD 344.72M crop damage). Fig. 4 provides a summary of all property and crop damage as well as injuries and fatalities caused by the six types of hazards in Miami-Dade County from 1979 to 2019. Hurricanes caused the highest property and crop losses as well as the highest number of fatalities in Miami-Dade County; however, heat resulted in the highest number of injuries. On the other hand, flooding caused more crop losses than property damage.

Figs. 5 and 6 show heatmap charts of flood-induced property and crop losses, respectively. For each flood event, the charts show the percentiles of all relevant hydrometeorological drivers (according to Fig. 2) and the damages caused in US Dollars. Heatmap charts for all other types of hazards are included in the Supplementary Material. Subsequent sections detail flood-related results only.

There were 30 property-damaging flood events in Miami-Dade County, of which 15 are found to be compound (Fig. 5) based on the 95th percentile threshold for hydrometeorological drivers that define compound events. The two most damaging events are compound events and collectively account for more than 99% of total property damage (~USD 800M). For these events, the percentiles of all four flooding drivers were very high as well (above the 98th percentile). Discharge and precipitation are found to largely drive compound flooding events precipitation and discharge exceeded the 95th percentile threshold five times. In the case of univariate events, precipitation was the main contributor to flooding, which exceeded the 95th percentile threshold in almost all univariate flood events except for only one case, where discharge was the only driver that exceeded the 95th percentile, causing USD 12,036 of property damage (Fig. 5). According to the NOAA Storm Events database, this event happened in October 2008, when intense rainfall occurred for over 4 h causing significant ponding of water and flooding. Poor drainage caused by clogged drains contributed to the flooding (NOAA NCEI 2021). Storm surge and soil moisture do not result in flooding themselves, but they were compounded with other flooding

The storm surge surpassed the threshold during five flooding events

and was always coincident with other drivers. High levels of soil moisture are not a univariate precondition; however, they can enhance the probability and severeness of flooding during extreme rainfall events. Soil moisture contributed to nine flooding events, but always in conjunction with other drivers (Fig. 5).

In addition, we assess whether flooding events were still causing property and crop damage when none of the drivers exceeded their individual 95th percentile thresholds. Two events, occurring in October 1991 and May 2000, had lower than 95th percentiles across all relevant drivers (rows marked with (N) in Fig. 5), but these events caused USD 47,570 and USD 7520 property damage, respectively.

Fig. 6 depicts a heatmap chart for crop damage caused by flooding in Miami-Dade County. Five events caused crop damage and four of those were compound events, causing 98.2% of the total losses. Precipitation was the primary contributor to all flooding events. One univariate event occurred in December 2000, where precipitation was the only variable above the 95th percentile threshold. In all four compound flooding events, discharge combined with precipitation to cause agricultural damage. Soil moisture was high in three of the events. There was only one instance where storm surge exceeded the threshold, and that happened when all other flooding drivers were also high. This event was Tropical Storm Leslie in October 2000, which caused by far the largest amount of crop damage.

5.1. Contributions of hydrometeorological drivers to compound events and their losses

Next, the contribution of each hydrometeorological driver to the identified compound events was assessed, for the six predominant hazard types responsible for the majority of losses in Miami-Dade County. Fig. 7 shows the total number of hazards, the number of events identified as compound, and how often different hydrometeorological drivers contributed to compound events. Results are shown for all events that caused socio-economic losses (property and crop damage, injuries, and fatalities) combined. Note that lightning, hail, and tornadoes are also included in Fig. 7 for hurricane, severe storm/thunderstorm, and winter weather; for the compound events in those hazard categories, we report the number of times lightning or tornadoes were present, as well as how often hail exceeded the severe probability threshold of 20%.

5.1.1. Flooding

Out of the 31 flood events, 16 were compound events (51.61%) and precipitation was a driver for each event (Fig. 7). The most frequent combination of compound drivers leading to flooding consisted of precipitation and river discharge (93.75%). In cases of univariate events (N = 13), precipitation was the most frequent driver (92.3%) leading to

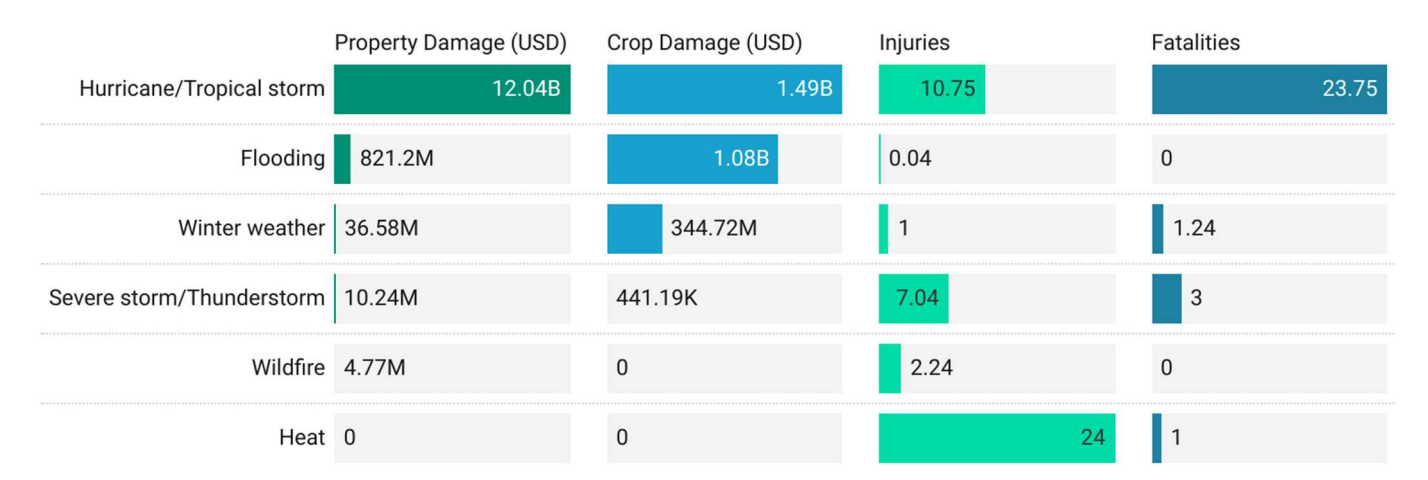


Fig. 4. Summary of direct losses, including property and crop damages as well as injuries and fatalities from all impactful events in Miami-Dade County corresponding to each hazard type (Data source: SHELDUS).

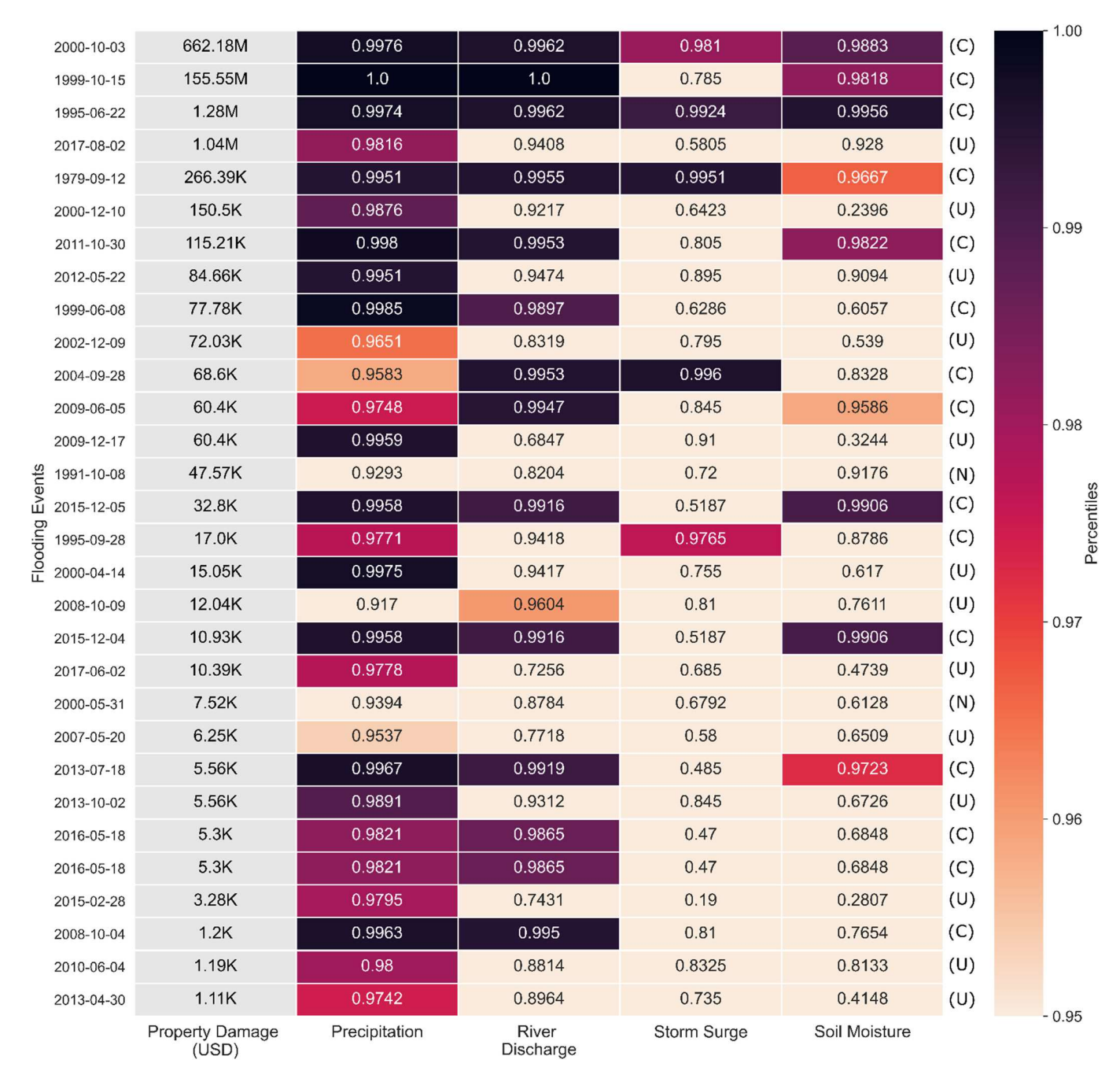


Fig. 5. Percentiles (in colored cells) of hydrometeorological variables (x-axis) corresponding to all flooding events that caused property losses (y-axis) in Miami-Dade County during 1979–2018. Events are sorted in descending order of property damage (in the left grey column). The letters C, U and N indicate compound events, univariate events, and events where none of the drivers exceeded the 95th percentile threshold, respectively. The color coding shows percentiles from 0.95 to 1.

flooding events, except for one event where river discharge was the only driver exceeding the threshold. River discharge contributed to 15 of the compound events, soil moisture to 10, and storm surge to 5 of them.

5.1.2. Hurricane/tropical storm

All hurricane/tropical storm events recorded in SHELDUS for Miami-Dade County (N=24) were compound events according to our definition (SI Figs. 2–4). Wind was the main contributor and often combined with river discharge (87.5%). Wind, river discharge, and storm surge compounded each other in 75% of the cases. Seven tornados occurred during hurricane events. One was above the Fujita scale of EF1 and six were above the Fujita scale of EF0. Lightning was present during 21 of the events. In 13 of those cases, the number of lightning strikes was

above 100.

5.1.3. Wildfire and heat

Four wildfire events were reported in SHELDUS and three of them were compound (SI Figs. 12 and 13). Soil moisture played a role in all of them, indicating the relevance of the pre-existing conditions for wildfires. Two of the three cases were composed of a high fire weather index (FWI) and low soil moisture. Conversely, only one out of four loss causing heat events were identified as compound (SI Figs. 10 and 11), where the maximum temperature and relative humidity both exceeded the threshold. There was no property or crop damage recorded for these heat events, but they did result in injuries and fatalities.

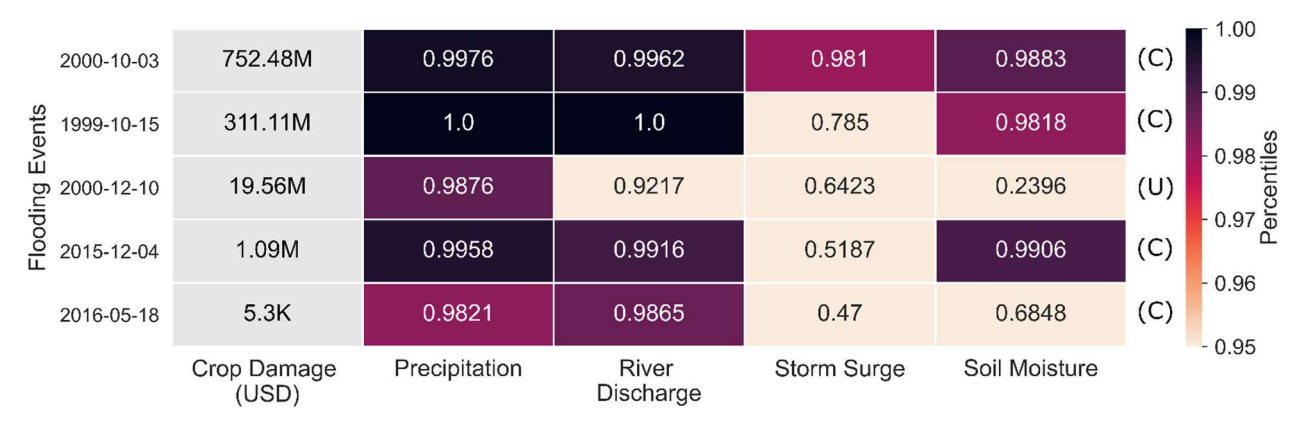


Fig. 6. Same as Fig. 5 but for crop damage.

5.1.4. Severe storms/thunderstorms

Severe storms/thunderstorms were compound in 23 events out of 63 (SI Figs. 6–9). Precipitation was the main contributor to these compound events (19 times), followed by river discharge (16 times). A tornado was reported during one of the compound events and lightning was present in 22 cases (note that lightning data is missing for one compound event). Soil moisture and wind surpassed the threshold 11 times during compound events and hail was present in 10 instances (note that hail data is missing for 6 of the compound events).

5.1.5. Winter weather

Nine winter weather events were reported in Miami-Dade County. Eight of them were compound events where both minimum temperature and wind always exceeded their respective thresholds.

6. Discussion

Damage resulting from natural hazards is influenced by hydrometeorological drivers and exposure, with drivers such as precipitation, temperature, and wind contributing to the severity of an event while exposure determines the extent of damage. The vulnerability of an area and its inhabitants to natural hazards is also critical in determining damage incurred. Matano et al. (2022) analyzed the socio-hydrological dynamics between drought and flood events using qualitative and semi-qualitative methods such as literature review, time series data analysis, stakeholder online survey, and semi-structured stakeholder interview. Our study does not estimate direct damage resulting from different hazards but primarily focuses on assessing the contributions of hydrometeorological drivers to the socio-economic losses of compound extreme events, and it does not consider dynamic changes in exposure and vulnerability. While these are important factors that may contribute to the impacts of extreme events, it is beyond the scope of our study. Nonetheless, we believe that our study provides valuable insights into the complex interplay between drivers and impacts, which can inform future research and practice in disaster risk reduction and climate adaptation.

Our analysis shows the contributions of different hydrometeorological drivers to the socio-economic impacts of six different hazard types in Miami- Dade County, Florida. This information is used to determine whether events were compound (i.e., multiple drivers exceeded their 95th percentiles simultaneously) or univariate. We found six types of natural hazards that have resulted in impacts in our study area. Precipitation was the major driver of flooding events which led to property and crop damage in Miami-Dade County. During the first two (from top) flooding events (i.e., October 2000 and October 1999) shown in Figs. 5 and 6, which were responsible for the highest property and crop damages, all hydrometeorological drivers were above their 98th percentiles (except for storm surge in the second most impactful crop damage event). These two flooding disasters resulted in the highest amount of

property loss in Miami-Dade County, as well as the highest crop loss. The flooding event of December 2000 also resulted in significant crop loss (USD 19.56 million), while property damage was much lower (USD 150.5K). All flooding occurrences that resulted in crop losses also added to property losses, albeit in different extents of damage.

We compare the locations identified in our analysis with the reports found in NOAA Storm Data publications. In the first event, on October 2/ 3, 2000, a broad low-pressure system off the southeast Florida coast moved northeast across central Florida and eventually became tropical storm Leslie off the northeast Florida coast. A band of heavy rain became nearly stationary across southeast Florida and produced a 10-mile-wide swath of 10-20 inches of rain in Miami-Dade County and southeast Broward County. Flooding of poorly drained urban areas quickly followed during the evening of October 3 and lasted into midday October 4 (NOAA Storm Events Database). Some floodwaters lingered for up to a week. Damage was particularly severe in the communities of Sweetwater, West Miami, Hialeah, Opa Locka and Pembroke Park (based on NOAA NCEI). Our results are consistent with the impact location reported in NOAA's National Centers for Environmental Information (NCEI) Storm Events reports. For the second event, there was widespread flooding from hurricane Irene that inundated most of the metropolitan areas of Miami-Dade, Broward, and Palm Beach counties and caused the second highest crop and property damages in Miami-Dade County. During this flooding event, precipitation, river discharge, and soil moisture were above their thresholds, while storm surge reached the 78th percentile. The grid point we identified with our framework as the most likely impact location is in the same area of damage described in the NOAA Storm Events Database. Out of the 31 flooding events in our study area, we found descriptive information on impact locations (including longitude/latitude values) in the NOAA's database for 16 events, and our results showed that 10 out of those 16 events were within 5 miles of the impacts reported in the NOAA database with an average of 10 miles considering all 16 events. Considering that impacts do not just occur at one single point, but typically across larger spatial areas, these results highlight the ability of our methodology to pinpoint the most likely area where impacts recorded in SHEL-DUS actually occurred.

It can be argued that river discharge and precipitation most often cooccur as a compound event. However, Fig. 8 shows that high precipitation and river discharge do not always occur together at the same location. For the costliest flooding event in Miami-Dade County (in the SHELDUS database), we found that sites of maximum percentiles of precipitation and river discharge are different from each other. It has also been shown that they are sometimes but not always significantly correlated with each other (Nasr et al., 2021).

We identify two events where none of the hydrometeorological drivers exceeded the 95th percentile threshold. One of them (the 14th event from the top in Fig. 5, which caused approximately USD 47,570 in property damage) occurred in October 1991 and according to the



Fig. 7. Contributions of different hydrometeorological drivers to compound extreme events in Miami-Dade County, FL. The charts show the overall number of events and total compound events for six different types of hazards (as classified in SHELDUS) that caused direct losses. The total number of compound events at the 95th percentile threshold is provided inside the charts. The numbers in the colored sections of the graphs show how often each driver surpassed the defined threshold (95th percentile) during compound events. Lightning, hail, and tornadoes are included in the case of Hurricane, Severe Storm/Thunderstorm, and Winter weather as the number of times lightning and tornadoes were present during compound events, as well as how often hail surpassed the severe probability of 20% during compound events. The numbers in brackets associated with Hail and Lightning indicate how many times data for hail and lightning were missing during compound events.

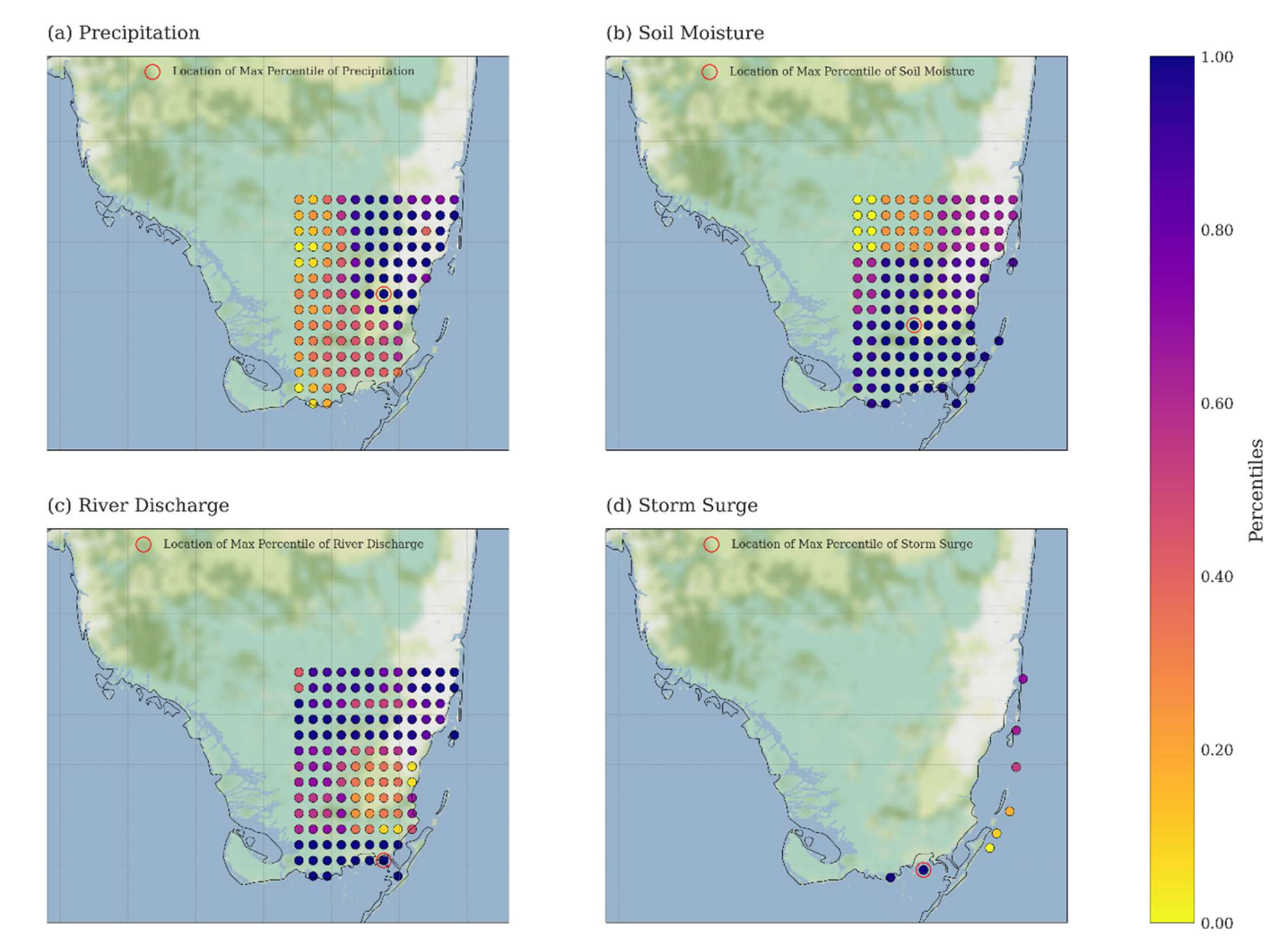


Fig. 8. Sites of maximum percentiles of flood drivers, (a) precipitation, (b) soil moisture, (c) river discharge, and (d) storm surge, during the costliest flooding event in Miami-Dade County in October 2000. The red circles indicate the sites of the maximum percentiles for each flood driver during the event.

description in NOAA Storm Events Database, heavy rain fell mostly in a narrow band from central Broward County across northern Miami-Dade County over a short time period of only a few hours, accumulating to 7–13 inches in southern Broward County, with lesser amounts in central Broward and northern Miami-Dade County, that resulted in flooded roads and homes. Although precipitation from that event did not exceed the 95th percentile threshold in Miami-Dade County, it was still high (~92nd percentile). It is also noted that we use daily precipitation data, which means that short-lived extreme events may not be captured well in these instances.

This paper proposes and implements a novel approach to analyze the contributions of different hydrometeorological drivers to the socioeconomic impacts of compound extreme events. Our results are consistent with previous studies that have analyzed the contributions of drivers to specific hazards such as flooding (e.g., Berghuijs et al., 2016; Tarasova et al., 2019). Our study expands on the previous research by considering a wider range of drivers and hazards and examining their compound effects on the resulting losses. By using a comprehensive dataset and a percentile-based approach to identify extreme events, our study provides valuable insights into the complex interplay between different drivers and their contributions to the socioeconomic impacts of compound extreme events.

The results provided in this work depend on the definition of "compound extreme", which in this case is the simultaneous exceedance above the 95th percentile. A sensitivity analysis was performed using

lower-end (90th) and higher-end (99th) percentile thresholds, to evaluate how the numbers of compound events and contributions of their drivers change (Table 3, SI Figs. 18 and 19). The sensitivity analysis was carried out for all events and for all locations in our study area. Fig. 5 shows two cases where none of the drivers were above the threshold (i. e., 95th percentile) but if we lower the threshold to the 90th percentile one becomes a univariate event and the other a compound event. For flooding, we identify 16 compound events if we consider the 95th percentile threshold, however, if we change the threshold to the 90th percentile the number of compound flooding events increases to 24. However, if the threshold is increased to the 99th percentile, the number of compound events decreases to 11. For example, the flooding event of October 1991 discussed above would in fact be considered a compound event if the 90th percentile threshold was used since precipitation and soil moisture values exceeded this threshold; this also shows that precipitation was the primary cause of this flooding event.

A sensitivity analysis using a lower-end (90th) percentile threshold and a higher-end (99th) percentile threshold to define compound events was carried out for all hazards. As expected, the number of identified compound events is sensitive to the choice of the threshold, but even when the threshold is increased to the 99th percentile (i.e., two drivers have to exceed that threshold to be classified as a compound event), we still find a significant percentage (more than 35% of total flooding events) of compound events (SI Fig. 19). For some hazard types, such as heat, wildfire, and winter weather, no compound events are identified

Table 3
Summary of compound events (threshold as 95th percentile) and their property and crop damage in Miami-Dade County, FL. In the parenthesis, results for sensitivity analysis (considering low-end (90th), and high-end (99th) percentiles) are shown.

Hazards	No. of events	Compound events (CEs)	Compound events (%)	Property loss by CEs (%)	Crop loss by CEs (%)
Flood	31	16 (24, 11)	51.61 (77.42, 35.48)	99.82 (99.99, 99.8)	98.2 (100, 98.2)
Hurricane	24	24 (24, 22)	100 (100, 91.67)	100 (100, 99.99)	100 (100, 100)
Wildfire	4	3 (4, 0)	75 (100, 0)	96.85 (100, 0)	NA
Heat	4	1 (1, 0)	25 <i>(25, 0)</i>	NA	NA
Severe storm/Thunderstorm	63	23 (38, 5)	36.51 <i>(60.32, 7.94)</i>	7.61 (12.12, 3.06)	82.15 (89.85, 0)
Winter weather	9	8 (8, 0)	88.89 (88.89, 0)	NA	100 (100, 0)

when considering the 99th percentile threshold.

When a high-end threshold (99th percentile) was used, the contributions of hydrometeorological drivers change making river discharge as the main driver exceeding the threshold in all compound events (N = 11) followed by precipitation in case of flooding hazard. Soil moisture contributed to 4 of the compound events, and storm surge to 3 of them. With a low-end threshold (90th percentile), however, precipitation is the dominant driver that exceeds the threshold in all compound flood events (N = 24), followed by river discharge that surpasses the threshold in 22 compound events. Soil moisture contributed to 13 of the compound events, and storm surge to 6 of them.

7. Conclusions

In this study, we developed a new bottom-up impact-based framework that combines historical socio-economic loss data from natural hazards reported in the SHELDUS database with multiple hydrometeorological datasets to assess the role of compound events in creating impacts. We also explored how different hydrometeorological drivers contribute to various types of climatic compound events.

The results show that over 50% of events from six types of natural hazards that occurred in Miami-Dade County were compound extreme events; these events account for over 80% of the recorded property and crop damages since 1979. Furthermore, based on our analysis, for three types of hazards: hurricanes, winter storms, and wildfires, nearly all events that caused damage were compound events. In contrast to past analyses, which typically explain compound events based on the dependence between two specific co-occurring variables, we show that historical compound extreme events in Miami-Dade County were often the result of more than two drivers and of different combinations of drivers.

The findings have broad-reaching implications from various perspectives. It provides crucial insights into which types of compound events are most prevalent as it relates to impacts in Miami-Dade County. We identify which drivers contribute to past natural hazards and their socio-economic losses. Compound events increase the challenge of climate adaptation for planners and decision-makers, as they often require different adaptation strategies than univariate events (e.g., a coastal flood barrier can prevent storm surge flooding but can also trap river discharge). In this context, our results provide information on the relative importance of compound events and which driver combinations most often led to impacts in the past. Furthermore, our results highlight the benefit of assessing compound extreme events from the perspective of recorded historical socio-economic impact data (rather than hypothesized models and/or assumptions), considering all relevant drivers, to quantify their contributions to past high-impact events. This can guide better disaster risk management and robust adaptation planning, as different types of hazards may require different types of solutions.

While our analysis uses the latest hindcast and reanalysis data available, it may not accurately represent observed climate extremes (e. g., extreme winds, river discharge) in all instances due to the spatial and temporal resolution. In addition, the SHELDUS dataset is known to underreport losses which could underestimate or overestimate the contribution of some events/drivers to the total reported damages. In the

future, it would be interesting to analyze how often two or more drivers of a particular hazard were extreme during time periods where no impacts were reported; this could be one way to assess underreported losses in the SHELDUS database. The framework that is introduced in this paper is transferable (where similar impact information is available) and scalable with the potential to further improve our understanding of compound events and their impacts.

Author contributions

Javed Ali (Conceptualization; Methodology; Data collection and curation; Software; Formal analysis; Investigation; Visualization; Writing-Original Draft; Writing-Review & Editing).

Alejandra R. Enriquez (Conceptualization; Methodology; Discussion; Writing - Review & Editing).

Md Mamunur Rashid (Conceptualization; Discussion; Review & Editing).

Joao Morim (Discussion; Review & Editing).

Thomas Wahl (Conceptualization; Methodology; Discussion; Writing - Review & Editing; Funding acquisition; Supervision).

Melanie Gall (Discussion; Review & Editing).

Christopher T. Emrich (Discussion; Review & Editing).

Declaration of competing interest

The authors declare that they have no known competing financial interests or personal relationships that could have appeared to influence the work reported in this paper.

Data availability

All hydrometeorological data used in this paper are publicly available (see Table 2). The socio-economic impacts data used in this study are not publicly available for legal/ethical reasons.

Acknowledgments

This work was supported by the United States National Academies of Sciences, Engineering and Medicine Gulf Research Program's Thriving Communities Grant (grant number: 200010880); the United States National Science Foundation (grant numbers: 2141461 and 2103754); and the European Union Horizon 2020 EXCELLENT SCIENCE - Marie Skłodowska-Curie Actions (grant number: 101019470 – SpaDeRisks https://cordis.europa.eu/project/id/101019470).

Appendix A. Supplementary data

Supplementary data to this article can be found online at https://doi. org/10.1016/j, wace. 2023. 100625.

References

Abatzoglou, J.T., 2013. Development of gridded surface meteorological data for ecological applications and modelling. Int. J. Climatol. 33 (1), 121–131. https://doi. org/10.1002/JOC.3413.

- AghaKouchak, A., Chiang, F., Huning, L.S., Love, C.A., Mallakpour, I., Mazdiyasni, O., Moftakhari, H., Papalexiou, S.M., Ragno, E., Sadegh, M., 2020. Climate extremes and compound hazards in a warming world. Ann. Rev. Earth Planet Sci. 48 (1), 519–548. https://doi.org/10.1146/annurev-earth-071719-055228.
- Berghuijs, W.R., Woods, R.A., Hutton, C.J., Sivapalan, M., 2016. Dominant flood generating mechanisms across the United States. Geophys. Res. Lett. 43 (9), 4382–4390. https://doi.org/10.1002/2016GL068070.
- Bevacqua, E., de Michele, C., Manning, C., Couasnon, A., Ribeiro, A.F.S., Ramos, A.M., Vignotto, E., Bastos, A., Blesić, S., Durante, F., Hillier, J., Oliveira, S.C., Pinto, J.G., Ragno, E., Rivoire, P., Saunders, K., van der Wiel, K., Wu, W., Zhang, T., Zscheischler, J., 2021. Guidelines for studying diverse types of compound weather and climate events. Earth's Future 9 (11). https://doi.org/10.1029/2021EF002340.
- Bevacqua, E., Maraun, D., Vousdoukas, M.I., Voukouvalas, E., Vrac, M., Mentaschi, L., Widmann, M., 2019. Higher probability of compound flooding from precipitation and storm surge in Europe under anthropogenic climate change. Sci. Adv. 5 (9), 1–8. https://doi.org/10.1126/sciadv.aaw5531.
- Bevacqua, E., Suarez-Gutierrez, L., Lehner, F., Vrac, M., Yiou, P., Zscheischler, J., Jezequel, A., 2022a. Advancing our understanding of compound weather and climate events via large ensemble model simulations. https://doi.org/10.21203/RS.3.RS-1791760/V1.
- Bevacqua, E., Zappa, G., Lehner, F., Zscheischler, J., 2022b. Precipitation trends determine future occurrences of compound hot-dry events. Nat. Clim. Change 12 (4), 350–355. https://doi.org/10.1038/s41558-022-01309-5, 2022 12:4.
- Camus, P., Haigh, I.D., Wahl, T., Nasr, A.A., Méndez, F.J., Darby, S.E., Nicholls, R.J., 2022. Daily synoptic conditions associated with occurrences of compound events in estuaries along North Atlantic coastlines. Int. J. Climatol. https://doi.org/10.1002/ JOC.7556.
- CEMHS, 2020. Spatial Hazard Events and Losses Database for the United States, Version 19.0. Center for Emergency Management and Homeland Security, Arizona State University, Phoenix, AZ [Online Database].
- CEMHS, 2022. Spatial Hazard Events and Losses Database for the United States, Version 20.0. Center for Emergency Management and Homeland Security, Arizona State University, Phoenix, AZ [Online Database].
- Chen, L., Yan, Z., Li, Q., Xu, Y., 2022. Flash flood risk assessment and driving factors: a case study of the Yantanxi river basin, southeastern China. Int J Disast Risk Sci 13 (2), 291–304. https://doi.org/10.1007/S13753-022-00408-3/FIGURES/5.
- Couasnon, A., Eilander, D., Muis, S., Veldkamp, T.I.E.E., Haigh, I.D., Wahl, T., Winsemius, H.C., Ward, P.J., 2020. Measuring compound flood potential from river discharge and storm surge extremes at the global scale. Nat. Hazards Earth Syst. Sci. 20 (2), 489–504. https://doi.org/10.5194/nhess-20-489-2020.
- Deng, D., Ritchie, E.A., 2019. An unusual extreme rainfall event in canberra Australia on february 2018. J. Geophys. Res. Atmos. 124 (8), 4429–4445. https://doi.org/ 10.1029/2019JD030420.
- Eilander, D., Couasnon, A., Leijnse, T., Ikeuchi, H., Yamazaki, D., Muis, S., Dullaart, J., Winsemius, H.C., Ward, P.J., 2022. A globally-applicable framework for compound flood hazard modeling. EGUsphere [Preprint]. https://doi.org/10.5194/egusphere-2022-149.
- $\label{lem:condition} Federal\ Emergency\ Management\ Agency.\ Natural\ Hazards\ \mid\ National\ Risk\ Index.\ FEMA\ (n.d.).\ https://hazards.fema.gov/nri/natural-hazards.$
- Hao, Z., Singh, V.P., Hao, F., 2018. Compound extremes in hydroclimatology: a review. Water (Switzerland) 10 (6), 16–21. https://doi.org/10.3390/w10060718.
- Harrigan, S., Zsoter, E., Barnard, C., Wetterhall, F., Ferrario, I., Mazzetti, C., Alfieri, L., Salamon, P., Prudhomme, C., 2021. River Discharge and Related Historical Data from the Global Flood Awareness System, v3.1, Copernicus Climate Change Service (C3S) Climate Data Store (CDS). https://doi.org/10.24381/cds.a4fdd6b9, 02/03/ 2021.
- Hersbach, H., Bell, B., Berrisford, P., Biavati, G., Horányi, A., Muñoz Sabater, J., Nicolas, J., Peubey, C., Radu, R., Rozum, I., Schepers, D., Simmons, A., Soci, C., Dee, D., Thépaut, J.-N., 2018. ERA5 Hourly Data on Single Levels from 1979 to Present. Copernicus Climate Change Service (C3S) Climate Data Store (CDS). https://doi.org/10.24381/cds.adbb2d47. (Accessed 2 March 2021).
- Hendry, A., Haigh, I.D., Nicholls, R.J., Winter, H., Neal, R., Wahl, T., Joly-Laugel, A., Darby, S.E., Joly-Lauge, A., Darby, S.E., 2019. Assessing the characteristics and drivers of compound flooding events around the UK coast. Hydrol. Earth Syst. Sci. 23 (7), 3117–3139. https://doi.org/10.5194/hess-23-3117-2019.
- Hirabayashi, Y., Tanoue, M., Sasaki, O., Zhou, X., Yamazaki, D., 2021. Global exposure to flooding from the new CMIP6 climate model projections. Sci. Rep. 11 (1), 1–7. https://doi.org/10.1038/s41598-021-83279-w, 2021 11:1.
- Ikeuchi, H., Hirabayashi, Y., Yamazaki, D., Muis, S., Ward, P.J., Winsemius, H.C., Verlaan, M., Kanae, S., 2017. Compound simulation of fluvial floods and storm surges in a global coupled river-coast flood model: model development and its application to 2007 Cyclone Sidr in Bangladesh. J. Adv. Model. Earth Syst. 9 (4), 1847–1862. https://doi.org/10.1002/2017MS000943.
- Jane, R., Cadavid, L., Obeysekera, J., Wahl, T., 2020. Multivariate statistical modelling of the drivers of compound flood events in south Florida. Nat. Hazards Earth Syst. Sci. 20 (10), 2681–2699. https://doi.org/10.5194/NHESS-20-2681-2020.
- Karl, T., Melillo, J., Peterson, T., 2009. Global Climate Change Impacts in the United States: a State of Knowledge Report from the U.S. Global Change Research Program. Cambridge University Press. http://hdl.handle.net/1834/20072.
- Kharin, V.V., Zwiers, F.W., Zhang, X., Wehner, M., 2013. Changes in temperature and precipitation extremes in the CMIP5 ensemble. Climatic Change 119 (2), 345–357. https://doi.org/10.1007/s10584-013-0705-8.
- Klaus, S., Kreibich, H., Merz, B., Kuhlmann, B., Schröter, K., 2016. Large-scale, seasonal flood risk analysis for agricultural crops in Germany. Environ. Earth Sci. 75 (18), 1–13. https://doi.org/10.1007/S12665-016-6096-1/FIGURES/6.

- Lawrence, M.B., Avila, L.A., Beven, J.L., Franklin, J.L., Pasch, R.J., Stewart, S.R., 2005. Atlantic hurricane season of 2003. Mon. Weather Rev. 133 (6), 1744–1773. https://doi.org/10.1175/MWR2940.1.
- Lenderink, G., Buishand, A., Van Deursen, W., 2007. Estimates of future discharges of the river Rhine using two scenario methodologies: direct versus delta approach. Hydrol. Earth Syst. Sci. 11 (3), 1145–1159. https://doi.org/10.5194/HESS-11-1145-2007.
- Leonard, M., Westra, S., Phatak, A., Lambert, M., van den Hurk, B., Mcinnes, K., Risbey, J., Schuster, S., Jakob, D., Stafford-Smith, M., 2014. A compound event framework for understanding extreme impacts. Wiley Interdiscip Rev: Clim. Change 5 (1), 113–128. https://doi.org/10.1002/wcc.252.
- Lian, J.J., Xu, K., Ma, C., 2013. Joint impact of rainfall and tidal level on flood risk in a coastal city with a complex river network: a case study of Fuzhou City, China. Hydrol. Earth Syst. Sci. 17 (2), 679–689. https://doi.org/10.5194/HESS-17-679-2013.
- Livneh, B., Rosenberg, E.A., Lin, C., Nijssen, B., Mishra, V., Andreadis, K.M., Maurer, E. P., Lettenmaier, D.P., 2013. A long-term hydrologically based dataset of land surface fluxes and states for the conterminous United States: update and extensions. J. Clim. 26 (23), 9384–9392. https://doi.org/10.1175/JCLI-D-12-00508.1.
- Mahdi El Khalki, E., Tramblay, Y., Massari, C., Brocca, L., Simonneaux, V., Gascoin, S., el Mehdi Saidi, M., 2020. Challenges in flood modeling over data-scarce regions: how to exploit globally available soil moisture products to estimate antecedent soil wetness conditions in Morocco. Nat. Hazards Earth Syst. Sci. 20 (10), 2591–2607. https://doi.org/10.5194/NHESS-20-2591-2020.
- Martius, O., Pfahl, S., Chevalier, C., 2016. A global quantification of compound precipitation and wind extremes. Geophys. Res. Lett. 43 (14), 7709–7717. https://doi.org/10.1002/2016GL070017.
- Masters, J., Henson, B., 2023. The U.S. Had 18 different billion-dollar weather disasters in 2022. Yale Climate Connections. Retrieved March 9, 2023, from. https://yaleclimateconnections.org/2023/01/the-u-s-had-18-different-billion-dollar-weather-disasters-in-2022/.
- Matanó, A., de Ruiter, M.C., Koehler, J., Ward, P.J., Van Loon, A.F., 2022. Caught between extremes: understanding human-water interactions during drought-to-flood events in the Horn of Africa. Earth's Future 10, e2022EF002747. https://doi.org/ 10.1029/2022EF002747.
- Matthews, T., Marston, G., 2019. How environmental storylines shaped regional planning policies in South East Queensland, Australia: a long-term analysis. Land Use Pol. 85, 476–484. https://doi.org/10.1016/J.LANDUSEPOL.2019.03.042.
- McPhillips, L.E., Chang, H., Chester, M.v., Depietri, Y., Friedman, E., Grimm, N.B., Kominoski, J.S., McPhearson, T., Méndez-Lázaro, P., Rosi, E.J., Shafiei Shiva, J., 2018. Defining extreme events: a cross-disciplinary review. Earth's Future 6 (3), 441-455. https://doi.org/10.1002/2017EF000686.
- Moftakhari, H., Schubert, J.E., AghaKouchak, A., Matthew, R.A., Sanders, B.F., 2019. Linking statistical and hydrodynamic modeling for compound flood hazard assessment in tidal channels and estuaries. Adv. Water Resour. 128 (September 2018), 28–38. https://doi.org/10.1016/j.advwatres.2019.04.009.
- Muis, S., Apecechea, M.I., Dullaart, J., de Lima Rego, J., Madsen, K.S., Su, J., Yan, K., Verlaan, M., 2020. A high-resolution global dataset of extreme sea levels, tides, and storm surges, including future projections. Front. Mar. Sci. 7, 263. https://doi.org/10.3389/FMARS.2020.00263/BIBTEX.
- Nakićenović, N., Swart, R., 2000. Special Report on Emissions Scenarios: a Special Report of Working Group III of the Intergovernmental Panel on Climate Change. htt ps://escholarship.org/uc/item/9sz5p22f.
- Nasr, A.A., Wahl, T., Rashid, M.M., Camus, P., Haigh, I.D., 2021. Assessing the dependence structure between oceanographic, fluvial, and pluvial flooding drivers along the United States coastline. Hydrol. Earth Syst. Sci. 25 (12), 6203–6222. https://doi.org/10.5194/hess-25-6203-2021.
- Nicholls, R., Hanson, S., Herweijer, C., Patmore, N., Hallegatte, S., Corfee-Morlot, J., Chateau, J., Muir-Wood, R., 2007. Ranking of the World's Cities Most Exposed to Coastal Flooding Today and in the Future. www.oecd.org.
- National Centers for Environmental Information (NCEI), 2021. National oceaninc and atmospheric administration (NOAA). Available at: https://www.ncdc.noaa.gov/stormevents/, 03/14/2022.
- NOAA National Centers for Environmental Information (NCEI) U.S, 2022. Billion-Dollar Weather and Climate Disasters. https://doi.org/10.25921/stkw-7w73. https://www.ncei.noaa.gov/access/billions/.
- NOAA National Centers for Environmental Information (NCEI) U.S, 2023. Billion-Dollar Weather and Climate Disasters. https://doi.org/10.25921/stkw-7w73. https://www.ncei.noaa.gov/access/billions/.
- NOAA National Centers for Environmental Information, 2022. Monthly National Climate Report for September published online October 2022, retrieved on November 10, 2022 from. https://www.ncei.noaa.gov/access/monitoring/monthly-report/nation al/202209/supplemental/page-5.
- Perkins, S.E., Alexander, L.V., 2013. On the measurement of heat waves. J. Clim. 26 (13), 4500–4517. https://doi.org/10.1175/JCLI-D-12-00383.1.
- Pierce, D.W., Su, L., Cayan, D.R., Risser, M.D., Livneh, B., Lettenmaier, D.P., 2021. An extreme-preserving long-term gridded daily precipitation data set for the conterminous United States. J. Hydrometeorol. 22 (7), 1883–1895. https://doi.org/ 10.1175/JHM-D-20-0212.1.
- Rashid, M.M., Wahl, T., 2022. Hydrologic risk from consecutive dry and wet extremes at the global scale. Environ. Res. Commun. 4 (7), 071001 https://doi.org/10.1088/ 2515-7620/ac77de.
- Raymond, C., Horton, R.M., Zscheischler, J., Martius, O., AghaKouchak, A., Balch, J., Bowen, S.G., Camargo, S.J., Hess, J., Kornhuber, K., Oppenheimer, M., Ruane, A.C., Wahl, T., White, K., 2020a. Understanding and managing connected extreme events. Nat. Clim. Change 10 (7), 611–621. https://doi.org/10.1038/s41558-020-0790-4.

- Raymond, C., Matthews, T., Horton, R.M., 2020b. The emergence of heat and humidity too severe for human tolerance. Sci. Adv. 6 (19) https://doi.org/10.1126/SCIADV. AAW1838/SUPPL_FILE/AAW1838_SM.PDF.
- Ridder, N.N., Pitman, A.J., Ukkola, A.M., 2022. High impact compound events in Australia. Weather Clim. Extrem. 36, 100457 https://doi.org/10.1016/J. WACE.2022.100457.
- Sadegh, M., Moftakhari, H., Gupta, H.v., Ragno, E., Mazdiyasni, O., Sanders, B., Matthew, R., AghaKouchak, A., 2018. Multihazard scenarios for analysis of compound extreme events. Geophys. Res. Lett. 45 (11), 5470–5480. https://doi.org/ 10.1029/2018GL077317.
- Seijas, N., Torriente, S.M., Hefty, N.L., Stults, M., Seijas, N., Torriente, S.M., Hefty, N.L., Stults, M., 2011. Preparing for climate change while advancing local sustainability: a closer look at miami-dade county, Florida, USA. Resilient Cities 503–513. https://doi.org/10.1007/978-94-007-0785-6 50.
- Seneviratne, S.I., Zhang, X., Adnan, M., Badi, W., Dereczynski, C., Di Luca, A., Ghosh, S., Iskandar, I., Kossin, J., Lewis, S., Otto, F., Pinto, I., Satoh, M., Vicente-Serrano, S.M., Wehner, M., Zhou, B., 2022. Weather and climate extreme events in a changing climate. In: Climate Change 2021: the Physical Science Basis. Contribution of Working Group I to the Sixth Assessment Report of the Intergovernmental Panel on Climate Change. https://doi.org/10.1017/9781009157896.013.
- Serafin, K.A., Ruggiero, P., Parker, K., Hill, D.F., 2019. What's streamflow got to do with it? A probabilistic simulation of the competing oceanographic and fluvial processes driving extreme along-river water levels. Nat. Hazards Earth Syst. Sci. 19 (7), 1415–1431. https://doi.org/10.5194/NHESS-19-1415-2019.
- Schipper, E.L.F., 2020. Maladaptation: when adaptation to climate change goes very wrong. One Earth 3 (4), 409–414. https://doi.org/10.1016/j.oneear.2020.09.014
- Simpson, N.P., Williams, P.A., Mach, K.J., Berrang-Ford, L., Biesbroek, R., Haasnoot, M., Segnon, A.C., Campbell, D., Musah-Surugu, J.I., Joe, E.T., Nunbogu, A.M., Sabour, S., Meyer, A.L., Andrews, T.M., Singh, C., Siders, A., Lawrence, J., van Aalst, M., Trisos, C.H., 2023. Adaptation to compound climate risks: a systematic global stocktake. iScience 26 (2), 105926. https://doi.org/10.1016/j. isci.2023.105926.
- Song, M., Jiang, X., Lei, Y., et al., 2023. Spatial and temporal variation characteristics of extreme hydrometeorological events in the Yellow River Basin and their effects on vegetation. Nat. Hazards 116, 1863–1878. https://doi.org/10.1007/s11069-022-05745-6.
- Sutanto, S.J., Vitolo, C., di Napoli, C., D'Andrea, M., van Lanen, H.A.J., 2020. Heatwaves, droughts, and fires: exploring compound and cascading dry hazards at the pan-European scale. Environ. Int. 134, 105276 https://doi.org/10.1016/J. ENVINT.2019.105276.
- Tarasova, L., Merz, R., Kiss, A., Basso, S., Blöschl, G., Merz, B., Viglione, A., Plötner, S., Guse, B., Schumann, A., Fischer, S., Ahrens, B., Anwar, F., Bárdossy, A., Bühler, P., Haberlandt, U., Kreibich, H., Krug, A., Lun, D., Wietzke, L., 2019. Causative classification of river flood events. Wiley Interdiscip Rev: Water 6 (4), e1353. https://doi.org/10.1002/wat2.1353.
- Tramblay, Y., Villarini, G., Khalki, E.M., Gründemann, G., Hughes, D., 2021. Evaluation of the drivers responsible for flooding in africa. Water Resour. Res. 57 (6), e2021WR029595 https://doi.org/10.1029/2021WR029595.
- United States Census Bureau, 2021. American Community Survey 5-Year Estimates. U.S. Census Bureau. American Community Survey Office. Web. 8 December 2022. htt
- van den Hurk, B.J.J.M., White, C.J., Ramos, A.M., Ward, P.J., Martius, O., Olbert, I., Roscoe, K., Goulart, H.M.D., Zscheischler, J., 2023. Consideration of compound drivers and impacts in the disaster risk reduction cycle. iScience, 106030. https:// doi.org/10.1016/j.isci.2023.106030.
- van den Hurk, B., van Meijgaard, E., de Valk, P., van Heeringen, K.J., Gooijer, J., 2015.

 Analysis of a compounding surge and precipitation event in The Netherlands.

- Environ. Res. Lett. 10 (3), 035001 https://doi.org/10.1088/1748-9326/10/3/035001
- Veatch, W., Villarini, G., 2020. Modeling the seasonality of extreme coastal water levels with mixtures of circular probability density functions. Theor. Appl. Climatol. 140 (3–4), 1199–1206. https://doi.org/10.1007/S00704-020-03143-1/FIGURES/4.
- Vitolo, C., di Giuseppe, F., Barnard, C., Coughlan, R., San-Miguel-Ayanz, J., Libertá, G., Krzeminski, B., 2020. ERA5-based global meteorological wildfire danger maps. Sci. Data 7 (1), 1–11. https://doi.org/10.1038/s41597-020-0554-z, 2020 7:1.
- Wahl, T., Jain, S., Bender, J., Meyers, S.D., Luther, M.E., 2015. Increasing risk of compound flooding from storm surge and rainfall for major US cities. Nat. Clim. Change 5 (12), 1093–1097. https://doi.org/10.1038/nclimate2736.
- Ward, P.J., Daniell, J., Duncan, M., Dunne, A., Hananel, C., Hochrainer-Stigler, S., Tijssen, A., Torresan, S., Ciurean, R., Gill, J.C., Sillmann, J., Couasnon, A., Koks, E., Padrón-Fumero, N., Tatman, S., Tronstad Lund, M., Adesiyun, A., Aerts, J.C.J.H., Alabaster, A., et al., 2022. Invited perspectives: a research agenda towards disaster risk management pathways in multi-(hazard-)risk assessment. Nat. Hazards Earth Syst. Sci. 22 (4), 1487–1497. https://doi.org/10.5194/NHESS-22-1487-2022.
- Ward, P.J., de Ruiter, M.C., Mård, J., Schröter, K., van Loon, A., Veldkamp, T., von Uexkull, N., Wanders, N., AghaKouchak, A., Arnbjerg-Nielsen, K., Capewell, L., Carmen Llasat, M., Day, R., Dewals, B., di Baldassarre, G., Huning, L.S., Kreibich, H., Mazzoleni, M., Savelli, E., et al., 2020. The need to integrate flood and drought disaster risk reduction strategies. Water Security 11, 100070. https://doi.org/10.1016/J.WASEC.2020.100070.
- World Meteorological Organization, 2023. Atlas of Mortality and Economic Losses from Weather, Climate and Water Extremes. Retrieved from. https://public.wmo.int/en/resources/atlas-of-mortality.
- World Economic Forum, 2023. The Global Risks Report 2023. Retrieved from. https://www.weforum.org/reports/global-risks-report-2023/in-full.
- Wu, W., McInnes, K., O'Grady, J., Hoeke, R., Leonard, M., Westra, S., 2018. Mapping dependence between extreme rainfall and storm surge. J. Geophys. Res.: Oceans 123 (4), 2461–2474. https://doi.org/10.1002/2017JC013472.
- Yaddanapudi, R., Mishra, A., Huang, W., Chowdhary, H., 2022. Compound wind and precipitation extremes in global coastal regions under climate change. Geophys. Res. Lett. 49 (15), e2022GL098974 https://doi.org/10.1029/2022GL098974.
- Zhang, W., Luo, M., Gao, S., Chen, W., Hari, V., Khouakhi, A., 2021. Compound hydrometeorological extremes: drivers, mechanisms and methods. Front. Earth Sci. 9, 673495 https://doi.org/10.3389/feart.2021.673495.
- Zheng, F., Westra, S., Leonard, M., Sisson, S.A., 2014. Modeling dependence between extreme rainfall and storm surge to estimate coastal flooding risk. Water Resour. Res. 50 (3), 2050–2071. https://doi.org/10.1002/2013WR014616.
- Zheng, F., Westra, S., Sisson, S.A., 2013. Quantifying the dependence between extreme rainfall and storm surge in the coastal zone. J. Hydrol. 505, 172–187. https://doi. org/10.1016/J.JHYDROL.2013.09.054.
- Zscheischler, J., Martius, O., Westra, S., Bevacqua, E., Raymond, C., Horton, R.M., van den Hurk, B., AghaKouchak, A., Jézéquel, A., Mahecha, M.D., Maraun, D., Ramos, A. M., Ridder, N.N., Thiery, W., Vignotto, E., 2020. A typology of compound weather and climate events. Nat. Rev. Earth Environ. 1 (7), 333–347. https://doi.org/10.1038/s43017-020-0060-z, 2020 1:7.
- Zscheischler, J., Seneviratne, S.I., 2017. Dependence of drivers affects risks associated with compound events. Sci. Adv. 3 (6), e1700263 https://doi.org/10.1126/sciadv.1700263
- Zscheischler, J., Westra, S., van den Hurk, B.J.J.M., Seneviratne, S.I., Ward, P.J., Pitman, A., AghaKouchak, A., Bresch, D.N., Leonard, M., Wahl, T., Zhang, X., 2018. Future climate risk from compound events. Nat. Clim. Change 8 (6), 469–477. https://doi.org/10.1038/s41558-018-0156-3.